

Computational Three-dimensional analysis of transport phenomena in a PEM fuel cell

K.Koteswararao ¹

1. M.Tech Student,

Mechanical Engineering department,

University College of Engineering,

JNTUK, Kakinada.

Dr. B. Balakrishna ²

2. Professor,

Mechanical Engineering department,

University College of Engineering,

JNTUK, Kakinada.

Abstract

A comprehensive non-isothermal, three-dimensional computational fluid dynamics model of a Polymer Electrolyte Membrane (PEM) fuel cell with serpentine gas flow channels has been developed. This comprehensive model accounts for important transport phenomena in a fuel cell such as heat transfer, mass transfer, electrode kinetics, and potential fields. Results obtained from this model reveal the detailed transport phenomena occurring inside the fuel cell such as reactant gas distributions, concentration of species, temperature distribution, potential distribution, and local current density distribution. The unique feature of this model is the implementation of the voltage-current algorithm that solves for the current density which allows for the calculation of the local activation over potentials

This present work deals with the thermodynamic modeling of a PEM fuel cell at various operating conditions through energy analysis. The correlations and equations available in literature were used to determine thermodynamic irreversibility in the PEM fuel cell at different operating conditions such as cell temperature, pressures of anode and cathode, current density, and membrane thickness as a design parameter.

1. Introduction

Limited resources of fossil fuels, increasing environmental pollution, rising costs of conventional fuels, and lower efficiency of conversion of energy in existing systems dictates the need of alternative way of power generation. Even though not mature fully, fuel cell is

foreseen as a potential alternative for power generation. Fuel cells have to compete with the other energy conversion devices such as gas turbines, gasoline engines and batteries.

A fuel cell is an electrochemical device which converts chemical energy of fuel and oxygen directly into electricity. A fuel cell is a battery-like device but unlike a battery it provides continuous electricity as long as fuel and oxygen are supplied. This technology is environment friendly, requires low maintenance for the component and high theoretical efficiency due to direct conversion of energy.

For the best performance of the fuel cell hydrogen is used as fuel and oxygen as the oxidant. Due to difficulties and risk associated with the use of hydrogen directly, other alternatives are used. Instead of direct hydrogen oil, methanol, natural gas etc. are used.

1.1 Proton Exchange Membrane Fuel Cell (PEMFC)

PEMFC is also called the Polymer electrolyte membrane fuel cell as the electrolyte used is a solid organic polymer. The material used consists of a fluorocarbon polymer backbone, the same as Teflon. The electrolyte is sandwiched between two graphite papers with the

catalyst spread in the interfaces. These two graphite papers are used as the anode and the cathode. Graphite papers, catalyst layers and the electrolyte together form the Membrane Electrode Assembly (MEA). On both the sides of MEA, graphite plates with grooves, which form the flow channels for hydrogen and oxygen, are attached. Figure: 1.2 shows the typical flow diagram of PEMFC.

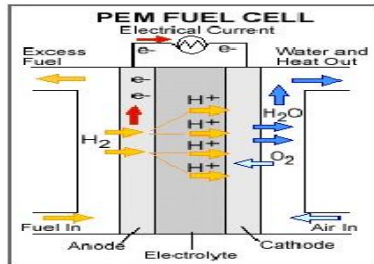
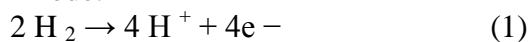
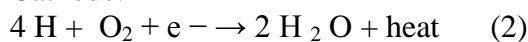


Fig. 1 Schematic Representation of PEMFC

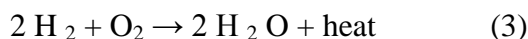
Anode:



Cathode:

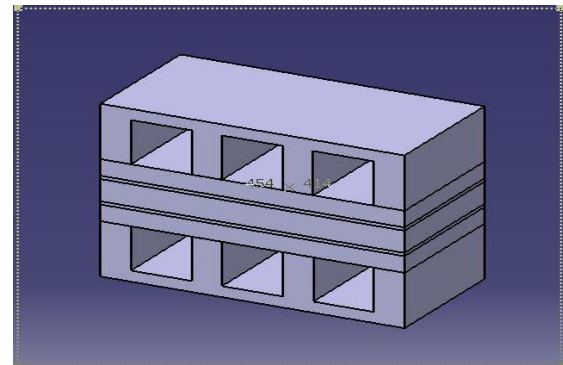


Overall reaction:



2. Fuel cell model:

The model presented here is a comprehensive fully three-dimensional, non-isothermal, single-phase, steady-state model that resolves coupled transport processes in the membrane, catalyst layer, gas diffusion electrodes, and reactant flow channels of a PEM fuel cell. The model features an algorithm that allows for a more realistic representation of the local activation over potentials, which leads to improved prediction of the local current density distribution.



2.1 Model Assumptions

1. The fuel cell operates under steady-state conditions
2. All gases are assumed to behave as ideal gases and fully saturated with water vapour, i.e. fully humidified conditions are assumed.
3. The gas mixture is assumed to be well mixed at the molecular level, with all components sharing the same velocity, pressure, and temperature fields.
4. The flow in the channels is considered laminar.
5. The membrane is assumed to be fully humidified and its ionic conductivity is taken to be constant.
6. Anode and cathode gases are not permitted to crossover, i.e. the membrane is impermeable.
7. The model is restricted to single-phase water transport in the gas diffusion electrodes and gas flow channels.
8. Water is assumed to be the product in the vapour phase, only consistent with the assumption of single-phase water transport.
9. The heat generation from the anode reaction is negligible and hence only cathode heat generation is considered.
10. Heat transfer inside the membrane is accomplished by conduction only.

3. Solution algorithm

The governing equations were discretized using a finite-volume method and solved using a general purpose CFD code. A computational mesh of 150 000 computational cells was found to provide sufficient spatial resolution. The solution begins by specifying a desired current density of the cell to use for calculating the

inlet flow rates at the anode and cathode sides. An initial guess of the activation over potential is obtained from the desired current density using the Butler–Volmer equation. Then follows the flow fields for velocities u , v , w , and pressure P . Once the flow field is obtained, the mass fraction equations are solved for the mass fractions of oxygen, hydrogen, water vapor, and nitrogen. Scalar equations are solved at last in the sequence of the transport equations for the temperature field in the cell and potential fields in the GDLs and the membrane. The local current densities are solved based on the Butler–Volmer equation. After the local current densities are obtained, the local activation over potentials can be readily calculated from the Butler–Volmer equation after one global loop.

3.1 Modeling parameters:

Table-1

parameter	Value (mm)
Channel Length (L)	50
Channel Height(H)	1
Channel Width(W_c)	1
Channel divider height	1
Channel divider Width	1
Electrode thickness(t_e)	0.26
Catalyst layer thickness(t_{cl})	0.0278
Membrane thickness(t_{mem})	0.23

3.2 Constant and Variable Parameters

Table-2

Parameter	Value
Cell temperature(T) in $^{\circ}K$	323;333;343;353
Cell pressure(P) in atm	3;4;5
Membrane(t_{mem}) thickness in mm	0.016;0.018;0.020
Current density(I) in A/cm^2	0.01-2.0
Anode stoichiometry(λ)	1.5
Cathode stoichiometry(ζ_A)	3.0
Anode transfer coefficient(α_A)	0.5

Cathode transfer coefficient(α_C)	1.0
Universal gas constant(R) in J/mol-K	8.314
Faraday's constant(F) in	96,485
Higher heating value of H_2 (HHV $_{H_2}$) in C/mol	286,000
Number of electrons involved (N)	2
Anode dry gas mole fraction(x_A)	0
Cathode dry gas mole fraction(x_C)	3.76
Electrode hydraulic permeability (k_p) in m^2	4.73E-19
Electrode thermal conductivity (λ_{eff}) in W/mK	1.3
Electrode electronic conductivity (Estimate) (λ_e) in S/m	570
Anode reference exchange current density($i_{o,a}^{ref}$) in A/cm^3	1.4E5
Cathode exchange current density ($i_{o,c}^{ref}$) in A/cm^3	1.0E-5

4.RESULTS& DISCUSSIONS:

4.1 Current Density Distribution

Figure 2 (a), (b), (c), (d) shows the current density distribution for four loading conditions. For low load condition, the effect of oxygen transport is small, i.e. the concentration of oxygen under the land area is still high, and therefore the current density is higher under the land area since the activation overpotential is higher under the land area. However, as the loading condition increases, the oxygen transport limitation under the land area become significant which results in the shift of current maxima towards the center of the channel where oxygen concentration is highest. The current density generally

decreases from inlet to outlet as the oxygen concentration decreases.

4.2 Oxygen Distribution

The detailed distribution of oxygen molar fraction for four different nominal current densities is shown in 2 (a), (b), (c), (d). In these cases, oxygen concentration decreases gradually with increasing of current densities from the

inlet flow channel to the outlet flow channel due to the consumption of oxygen at the catalyst layer. In the GDL, oxygen concentration under the land area is smaller than that under the channel area. The concentration of oxygen at the catalyst layer is balanced by the oxygen that is being consumed and the amount of oxygen that diffuses towards the catalyst layer driven by the concentration gradient. The lower diffusivity of the oxygen along with the low concentration of oxygen in ambient air results in noticeable oxygen depletion under the land areas. At a low current density, the oxygen consumption rate is low enough not to cause diffusive limitations, whereas at a high current density the concentration of oxygen under the land areas has already reached near-zero values. In addition, the local current density of the cathode side reaction depends directly on the oxygen concentration.

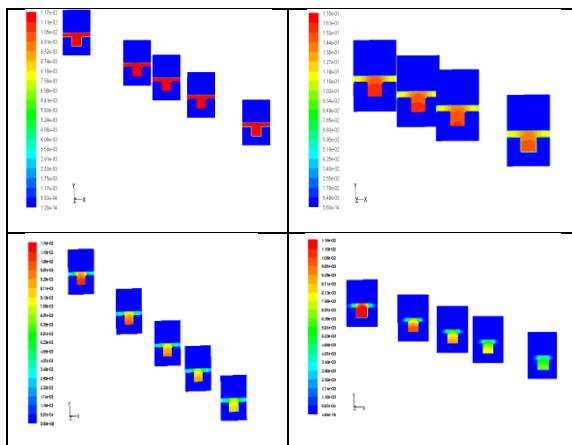


Fig 2 (a), (b) (c), (d) **Oxygen** molar fraction distribution in the cathode side for

loading conditions: $0.17 \frac{A}{cm^2}$, $0.673 \frac{A}{cm^2}$, $1.3 \frac{A}{cm^2}$, $1.9 \frac{A}{cm^2}$

4.3 Hydrogen Distribution

The hydrogen molar fraction distribution in the anode side is shown in fig 3 (a), (b), (c), (d) for four nominal current densities. In general, the

hydrogen concentration decreases from inlet to outlet as it is being consumed. However, the decrease is quite small along the channel and the decrease in molar concentration of the hydrogen under the land areas is smaller than for the oxygen in the cathode side due to the higher diffusivity of the hydrogen.

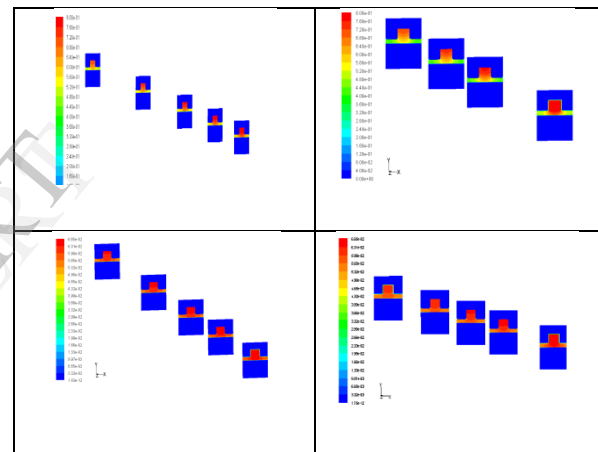


Fig 3(a) (b), (c), (d) Hydrogen molar fraction distribution in the anode side for three loading conditions: $0.173 \frac{A}{cm^2}$, $0.673 \frac{A}{cm^2}$, and $1.3 \frac{A}{cm^2}$, $1.29 \frac{A}{cm^2}$

4.4 Water Distribution:

The water molar fraction distribution in the cell is shown in Fig 4(a), (b), (c), (d) for four different nominal current densities. Significant condensation is expected to occur under the cathode land area for all nominal current densities. However, the magnitude of water mole fractions is higher for high nominal current density than for low current density.

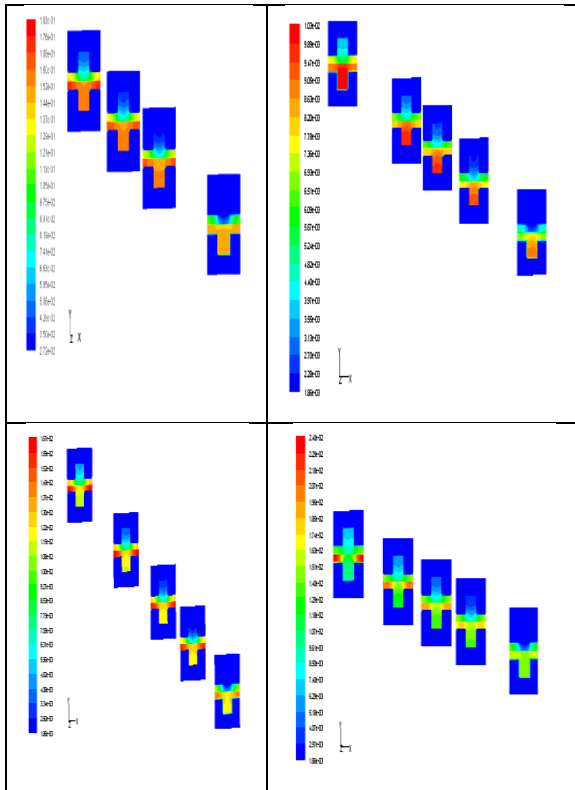


Fig 4(a), (b), (c), (d) Water molar fraction distribution for the loading conditions: 0.173 A/cm^2 , 0.673 A/cm^2 , 1.3 A/cm^2 and 1.9 A/cm^2 .

4.5 Current density Distribution in the Cathode side Gas diffusion Layer

Figure 5 (a), (b) shows that the current density distribution patterns for all loading conditions. However, the magnitude of the potential loss increases with cell loading for low load condition current density is very high and high load condition current density distribution is decreases. In the GDLs oxygen is consumption with the high load condition for that electron transport in gas diffusion layer is resist to increase the voltage losses these losses are ohmic over potential in the gas diffusion layer it mainly in cathode side because the reaction takes place only in the cathode side.

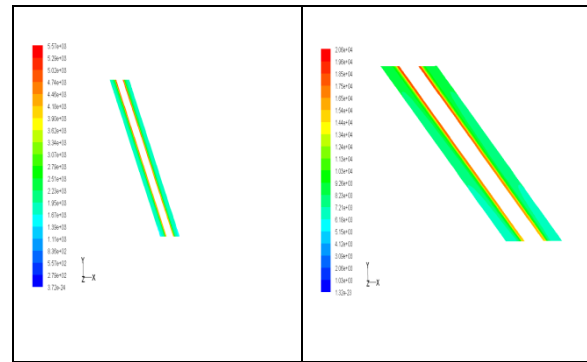


Fig 5. (a),(b) Current density distribution of cathode side gas diffusion layer at cell potential $v=0.845\text{V}$, $v=0.69\text{V}$

4.6 Current density Distribution in the Cathode Catalyst Layer

Figure 6(a), (b),(c) shows that cathode current density distribution in the first sub-layer (GDL/catalyst layer) of the catalyst layer. In all loading conditions, the distribution patterns of current density are similar, with higher loading conditions under the land area. This uneven distribution is mainly due to lower Ohmic loss under the channel area. Since current density has an exponential effect on the over potential. It can be deduced that the potential condition for producing current under the land area is more favorable in the absence of oxygen transport limitation.

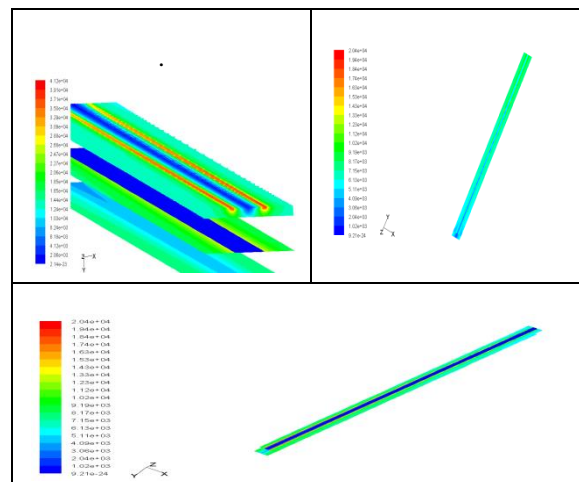


Fig 6. (a), (b) (c) Current density distribution of cathode side catalyst layer at cell potential $v=0.62\text{V}$, $v=0.62\text{V}$, $v=0.745$

5. Design Parameters and Material Properties:

5.1 Effect of membrane thickness:

In Fig. 7 plot is drawn between Irreversible voltage Vs current density and Energy Efficiency Vs current density when cell is operated at $P = 3$ atm, $T = 353$ K and the membrane thickness is varied as 0.016 cm, 0.018 cm, 0.020 cm. We can observe from the above plot, the irreversible voltage is increasing with increase in current density where as energy efficiency is decreasing with increase in

current density for a given temperature, pressure, membrane thickness. We can also observe that the irreversible voltage is increasing and energy efficiency is decreasing with increase in membrane thickness. In order to decrease thermodynamic irreversibility's in the cell, and thus, to increase the net generated power per area and efficiency of PEM fuel cell, it is suggested that the lower membrane thickness should be selected in case the PEM fuel cell when operated under constant cell operating temperature and pressure.

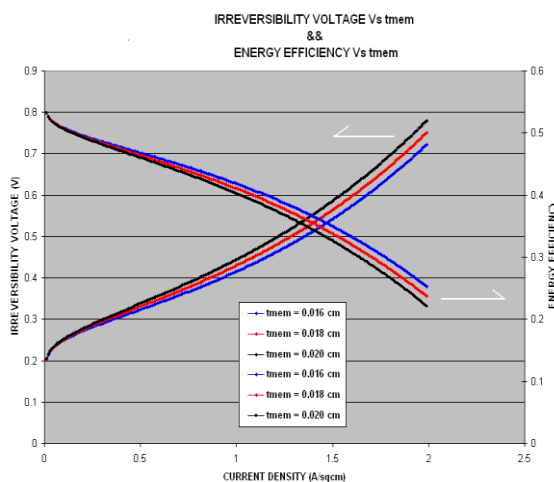


Fig7 Irreversibility Voltage, Energy Efficiency Varying with thickness of membrane

5.2 Effect of temperature:

In Fig. 8 plot is drawn between Irreversible voltage Vs current density and Energy Efficiency Vs current density when cell is operated at $P = 3$ atm, thickness of membrane = 0.018 cm and the cell temperature is varied as 323 K, 333 K, 343 K, 353 K. We can observe that the irreversible voltage is decreasing and energy efficiency is increasing with increase in temperature. In order to decrease thermodynamic irreversibility's in the cell, we have to increase the net generated power per area and efficiency of

PEM-fuelcell.

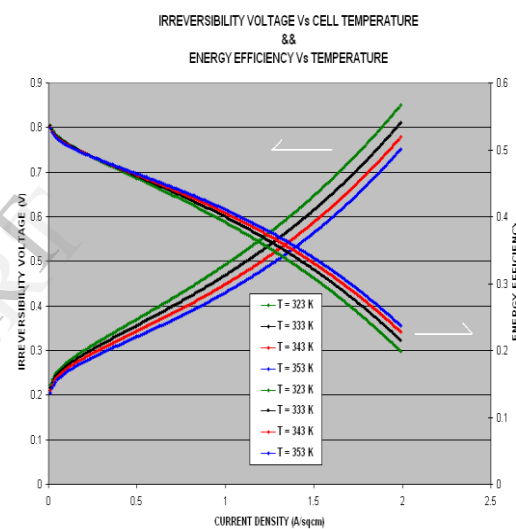


Fig.8. Irreversibility Voltage, Energy Efficiency Varying with Cell Temperature.

5.3 Effect of pressure:

In Figure 9 , plot is drawn between Irreversible voltage Vs current density and Energy Efficiency Vs current density when cell is operated at $T = 353$ K, thickness of membrane = 0.018 cm and the cell pressure is varied as 3 atm, 4 atm, 5 atm. We can observe that the irreversible voltage is decreasing and energy efficiency is increasing with increase in pressure.

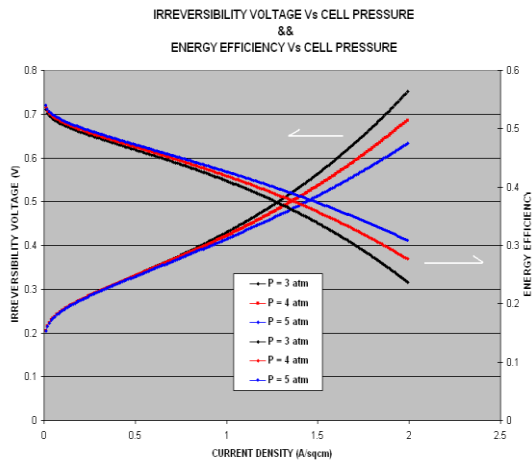


Fig. 9 Irreversibility Voltage, Energy Efficiency Varying with Cell Pressure

6. Conclusions

A three-dimensional computational fluid dynamics model of PEM fuel cell with serpentine flow channels was developed in this work. The unique feature of this model is the implementation of the voltage-to-current (VTC) algorithm that allows for the calculation of the electrochemical kinetics without simplifications. This calculation involves the coupling of the potential field with the reactant species concentration field which results in an accurate prediction of local current density distribution. Furthermore, the current density distribution patterns vary with load conditions. At low load, the current density is higher in the land area and as the load is increased, the current density maximum shifts towards the centre of the channel. These local current density distribution patterns are radically different from those obtained with models that do not account for the non-uniformity of surface overpotential. The results show that at moderate and high load conditions, most of the activity occurs at the first catalyst sub-layer adjacent to the GDL.

In addition to revealing the detail information about the transport phenomena inside the fuel cell, this model

was applied to investigate the sensitivity of various operating and material parameters on fuel cell performance. The results of these studies show that fuel cell perform better at higher temperature, pressure, and electrode porosity, conductivity with membrane water content.

iii. Expansion of the computational domain from one serpentine turn to a single cell that has many turns. This would be very computationally demanding and would require a code that can support parallel processing.

iv. Extension of the model from steady state to transient

7. references

- [1] F. Barbir, J. Braun, and J. Neutzler. "Properties of Molded Graphite Bi-Polar Plates for PEM Fuel Cell Stacks", *Journal of New materials for Electrochemical Systems*, 2:197-200, 1999.
- [2] D.M. Bernardi and M.W. Verbrugge. "Mathematical Model of a Gas Diffusion Electrode Bonded to a Polymer Electrolyte". *AIChE Journal*, 37(8): 1151-1162, 1991.
- [3] D. M. Bernadi and M. W. Verbrugge. "A Mathematical Model of the Solid-Polymer-Electrolyte Fuel Cell". *J. Electrochem. Soc.*, 139(9): 2477-2491, 1992.
- [4] T. Berning "Three-Dimensional Computational Analysis of Transport Phenomena in a PEM Fuel Cell". PhD Thesis, 2002.
- [5] T. Berning, D.M. Lu, N. Djilali. "Three-Dimensional Computational Analysis of Transport Phenomena in a PEM Fuel Cell". *Journal of Power Sources*, 106: 284-294, 2002.
- [6] R.B. Bird, W. Steward, and E. N. Lightfoot. "Transport Phenomena". Wiley, New York, 1960.
- [7] F.N. Buchi, and S. Srinivasan. "Operating Proton Exchange Membrane

Fuel Cells without External Humidification of the Reactant Gases". J. Electrochem. Soc., 144(8): 2767-2772, 1997.

[8] S. Chintada, K-H KO, and N. K. Anand. "Heat Transfer in 3-D Serpentine Channels with right-Angle Turns". Numerical Heat Transfer, Part A, Vol. 36, 781-806, 1999.

[9] J.M. Choi and N.K. Anand. "Heat Transfer in a Serpentine Channel with a Series of Right-Angle Turns". Numerical Heat Transfer, Part A., Vol. 23, 189-210, 1993.

IJERT